Materials and Design 145 (2018) 218–225

Contents lists available at ScienceDirect

Materials and Design

journal homepage: www.elsevier.com/locate/matdes

Adhesion force measured by atomic force microscopy for direct carbon fiber-epoxy interfacial characterization

Nan Zheng [a,b], Jinmei He [a,c,*], Jiefeng Gao [d], Yudong Huang [a], Flemming Besenbacher [c], Mingdong Dong [c,**]

[a] MIIT Key Laboratory of Critical Materials Technology for New Energy Conversion and Storage, State Key Laboratory of Urban Water Resource and Environment, School of Chemistry and Chemical Engineering, Harbin Institute of Technology, Harbin 150001, China
[b] School of Light Industry and Chemical Engineering, Dalian Polytechnic University, Dalian 116034, China
[c] Interdisciplinary Nanoscience Center (iNANO), Aarhus University, 8000 Aarhus, Denmark
[d] College of Chemistry and Chemical Engineering, Yangzhou University, Yangzhou 225009, China

HIGHLIGHTS

- A novel technique to study the interfacial adhesion in carbon fiber/epoxy composite by atomic force microscopy was proposed.
- The adhesion forces between three types of carbon fibers and epoxy functionalized tip were measured.
- Adhesion force results demonstrate the direct effect of surface chemistry of carbon fiber on the interfacial adhesion.
- Adhesion force measurement has excellent correlation with single fiber microbond test on the carbon fiber/epoxy composite.

GRAPHICAL ABSTRACT

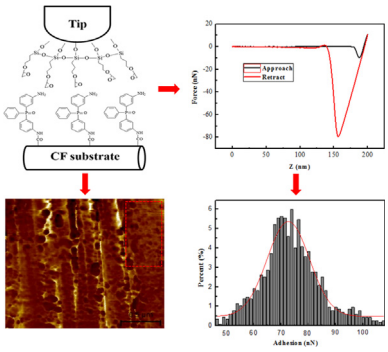

ARTICLE INFO

Article history:
Received 17 November 2017
Received in revised form 19 February 2018
Accepted 20 February 2018

Keywords:
Atomic force microscopy
Tip functionalization
Carbon fiber
Epoxy
Adhesion force

ABSTRACT

Adhesion force measurement by Atomic force microscopy (AFM) is used to investigate the interfacial interaction of the carbon fiber (CF)/epoxy composite for the first time. The epoxy functionalized AFM tip and three types of carbon fibers with different surface chemistry and morphologies were used in this study. Results show that the Bis (3-aminophenyl) phenyl phosphine oxide (BAPPO) modified CF possesses a much larger adhesion force (72.7 nN) than the as-received and de-sized CF (22.5 nN and 17.9 nN, respectively) due to formation of the chemical bonding between the BAPPO modified CF and the epoxy functionalized tip. Single fiber microbond test demonstrates that the interfacial shear strength (IFSS) of BAPPO modified CF/EP composite is 15% and 22% larger than that of as-received and de-sized CF/EP, respectively. This nanoscale manipulation by AFM provides a new avenue to measure the interfacial adhesion between the CF and epoxy at the molecular level.

* Correspondence to: J. He, MIIT Key Laboratory of Critical Materials Technology for New Energy Conversion and Storage, State Key Laboratory of Urban Water Resource and Environment, School of Chemistry and Chemical Engineering, Harbin Institute of Technology, Harbin 150001, China.
** Corresponding author.
E-mail addresses: hejinmei@hit.edu.cn (J. He), dong@inano.au.dk (M. Dong).

https://doi.org/10.1016/j.matdes.2018.02.060
0264-1275/

1. Introduction

Carbon fiber reinforced epoxy composites have attracted considerable attention from both academia and industry due to their superior specific strength and elastic modulus [1,2]. As known, the mechanical properties of fiber-reinforced composites are not only influenced by the intrinsic characteristics of the fiber and matrix but also depend on the interfacial adhesion between the reinforcing CF and the resin matrix. Excellent interfacial adhesion is essential to ensure efficient load transfer from matrix to fibers, which can reduce stress concentrations and thus improve the overall mechanical properties. So far, various techniques including fiber pull-out [3–5], fiber push-out [6,7], and fiber fragmentation [8–11], have been used to characterize the interfacial adhesion between the fiber and matrix. These techniques can provide a lot of information about interfacial interactions such as the interfacial shear strength (IFSS) and the critical energy release rate, G_{IC}. However, both the sample fabrication and measurement are tedious. Therefore, it is desirable to develop a direct and novel technique to obtain the interfacial adhesion force and understand the adhesion mechanism between fibers and matrix especially at the molecular level.

Atomic force microscopy (AFM) is commonly considered as a powerful tool for imaging the nanoscale topography of materials and recording the mechanical, electrical, piezoelectrical, magnetic and chemical properties of sample surfaces [12–15]. Recently, a kind of novel AFM imaging mode, namely, PeakForce Quantitative Nanomechanical Property Mapping (QNM), was introduced for both the topography imaging with a high resolution and accurate measurement of nanomechanical properties of the substrate including modulus, deformation and dissipation [16]. In addition, this technique allows quantifying adhesion forces between the AFM tip and substrate under different environmental conditions [17]. In such an experiment, the substrate is scanned by a tip mounted on a cantilever spring. When the tip first approaches and then retraces from the substrate, the force between the tip and the substrate is measured by monitoring the deflection of the cantilever.

When the AFM tip is chemically functionalized, the adhesion force obtained can reflect the chemical interaction between specific molecules on the functionalized tip and the target substrate, which has found wide applications in biological fields, surface science and material science [18,19]. For example, D. Alsteens et al. [18] applied AFM with hydrophobic tips for directly measuring the local hydrophobic forces on organic surfaces, and found the nanoscale AFM measurement had an excellent correlation with the macroscale wettability measurements. M.A. Poggi et al. [20] examined the adhesion between thiolated AFM cantilever tips and the single walled carbon nanotube paper using a chemical force microscopy and observed a direct correlation of adhesion force with respect to the thiol terminal group on the AFM cantilever tips ($NH_2 > CH_3 > OH$). Based on the above discussion, it is expected that the adhesion force measurement by AFM can also applied in the fiber-reinforced composite to study the interfacial interaction between the epoxy and CF from the molecular level, which was, however, never reported in the open literatures.

In this paper, the interaction force between carbon fiber and epoxy was measured by using the AFM tip modified with (3-glycidyloxypropyl) trimethoxysilane. Three types of CFs were chosen as the substrate for the adhesion force measurement, and their morphologies, surface chemical composition and surface energy were analyzed by AFM, X-ray photoelectron spectroscopy and dynamics contact angle test, respectively. In addition, a traditional single fiber microbond test was also performed to verify the results obtained from the adhesion force measurement.

2. Experimental work

2.1. Materials

T300 polyacrylonitrile-based carbon fiber was used in this research and their parameters provided by the manufacturer of ToRay Ltd., Japan are listed below: tensile strength: 3.5 GPa, density: 1.8 g/cm^3, and diameter: 6.5 μm. The epoxy resin (E-51) and curing agent (H-256) were provided by Shell Chemical Corporation. (3-Glycidyloxypropyl) trimethoxysilane (98%) and thionyl chloride were purchased from Sigma-Aldrich, USA. Triphenylphosphine oxide (98%) and hydrazine hydrate (98%) were obtained from Aladdin Reagent Corp. (Shanghai, China) and TCI Ltd., Japan, respectively. Pd/C catalytic agent (5%), concentrated sulfuric acid (95–98%) and nitric acid (68%) were provided by Sinopharm Chemical Reagent Co., Ltd., China. All chemical reagents and solvents were used as received and without further purification.

2.2. Preparation of three types of carbon fibers

i) *as-received CF sample*: As known, the as-received T300 carbon fiber was covered by a layer of commercial epoxy sizing agent on its surface.
ii) *de-sized CF sample*: The as-received CF was refluxed in acetone at 70 °C for 48 h to remove the surface sizing agent and other contaminants, and the obtained CF was denoted as 'de-sized CF'.
iii) *BAPPO-CF sample*.

Bis(3-aminophenyl) phenyl phosphine oxide (BAPPO) was synthesized in two steps. At the first step, triphenyl phosphine oxide (13.9 g, 0.05 mol) was stirred in a 250 ml round-bottom flask in a nitrogen atmosphere. Then 96% sulfuric acid (100 ml) was added. When the reactants were dissolved and cooled to −5 °C in an ice/salt bath, a mixed solution of fuming nitric acid (5.2 ml) and sulfuric acid (50 ml) was added dropwise over a period of 2 h. Then, the mixed solution was maintained at room temperature for 8 h followed by adding 1 l of ice into the solution for hydrolysis. When the ice was melted, the mixture was extracted with chloroform and rinsed with sodium bicarbonate aqueous solution until neutral pH. At last, BNPPO with a 70% yield was obtained after removing the solvent and recrystallizing the solid residue from absolute ethanol.

The second step was conducted in a 250 ml round-bottom flask containing the as-prepared BNPPO (14.3 g, 0.04 mol), absolute ethanol (100 ml) and catalytic agent Pt/C (0.5 g). When the reaction temperature reached 80 °C, 80% $N_2H_4 \cdot H_2O$ solution (65 ml) was added dropwise over a period of 1 h. Then, the reaction was maintained at 80 °C for another 24 h. Subsequently, the Pt/C and solvent was removed by filtration and vacuum distillation, respectively. After the recrystallization from 50% ethanol, BAPPO with an 80% yield was finally obtained.

Before the introduction of BAPPO, the de-sized CFs were firstly oxidized in the concentrated nitric acid (HNO_3) at 80 °C for 3 h to obtain the carboxyl functionalized carbon fibers (COOH-CF). The COOH-CF further reacted with a mixture of 100 ml thionyl chloride and 5 ml dimethyl formamide at 80 °C for 48 h to obtain the acyl chloride functionalized carbon fibers (COCl-CF). The BAPPO modified CFs were subsequently prepared by the reaction of COCl-CF with a mixed solution of BAPPO (2.8 g), dimethyl formamide (100 ml) and triethylamine (5 ml) at 120 °C for 24 h. Through the above steps, 3 wt% of BAPPO was introduced onto the de-sized CF surfaces (coded as BAPPO-CF).

2.3. Adhesion force measurement

Adhesion force measurement between CF substrate and epoxy functionalized AFM tip was performed in a commercial Nanoscope VIII MultiMode SPM system (Bruker, Santa Barbara, CA) with Peak Force Tapping mode at room temperature and a relative humidity of 40–60%. Epoxy functionalized AFM tip was obtained by treating the as-received silicon nitride AFM tip (SCANASYST-AIR) with (3-glycidyloxypropyl) trimethoxysilane [21]. Specifically, the as-received AFM tip was first immersed into a standard piranha solution of H_2SO_4/

H_2O_2 (70:30 (v/v)) for a couple of seconds and then thoroughly rinsed with deionized water and ethanol. Subsequently, the tip was dipped into 0.5% (3-glycidyloxypropyl) trimethoxysilane/toluene solution for silanization, and epoxy functionalized tip was finally obtained after it was washed by toluene, CH_2Cl_2 and ethanol and then dried under nitrogen for 4 h.

A schematic illustration of the typical measurement of the adhesion force between the epoxy functionalized tip and BAPPO modified CF is shown in Fig. 1(a). The BAPPO modified CF monofilament served as the substrate was glued onto an iron flake using the double-side tape. When the tip approaches and retracts from the CF substrate at a constant rate of 1 μm/s, a force-displacement curve could be in-situ recorded by monitoring the deflection of the cantilever using optical lever technique. The sensitivity of the optical lever detection was measured by indenting the AFM tip into a hard surface. For further details on AFM force spectroscopy, see reference [22]. Fig. 1(b) displays a typical relation between the adhesion force and the tip distance during the adhesion force measurement. When the AFM tip attached on a cantilever is far from the CF surface, there is no force detected. As the tip approaches to the surface, the attractive forces such as van der Waals forces appear [23]. When the tip continues to press into the surface until a pre-defined point, the cantilever is retracted, and the tip is detached from CF surface once the retractive force from the spring exceeds the adhesion forces [24]. Here, the maximum force for separating the tip with the CF substrate is regarded as the adhesion force between the CF and the epoxy functionalized tip, which can be calculated based on the cantilever's spring constant of 0.4 N/m and the deflection of the cantilever [25]. The offline software of NanoScope Analysis (Bruker, Santa Barbara, CA) was used for analyzing all of the force-distance curves and the average adhesion force was determined by fitting a Gaussian profile to the histogram of forces. For comparison, the tests based on the as-received CF or de-sized CF as the substrates were also performed.

2.4. Materials characterization and IFSS test

Fourier transform infrared (FTIR) spectra were recorded using a Nicolet-Nexus 670 spectrophotometer with a potassium bromide pellet. ^{1}HNMR spectra were obtained with a Bruker MSL-300 (300 MHz) NMR spectrometer with $CDCl_3$ as a solvent. X-ray photoelectron spectroscopy (XPS) spectra were taken using a Thermo ESCALAB 250 photoelectron energy spectrometer equipped with AlK X-ray source (1486.6 eV), where the binding energy scale was calibrated by C1s (284.6 eV) and the X-ray power was set at 200 W.

Table 1
Surface free energy characteristics of the liquids.

Liquid	γ (mN/m)	γ^d (mN/m)	γ^p (mN/m)
Water	72.8	21.8	51.0
Ethylene glycol	48.3	29.3	19.0

Dynamic contact angle tests were conducted on a dynamic contact angle meter (DCAT21, Data Physics Instruments, Germany) and performed at a motor speed of 0.01 mm/s and the fiber immersion depth was controlled at 5 mm in the test liquids. Two types of liquids with different polar and dispersive components of the surface energy were used for the test, as presented in Table 1. Fowkes model was used for determining the surface energy from the contact angle data [26], as shown in Eqs. (1) and (2):

$$\gamma_l (1+\cos\theta) = 2\left(\gamma^d{}_l \gamma^d{}_f\right)^{1/2} + 2\left(\gamma^p{}_l \gamma^p{}_f\right)^{1/2} \quad (1)$$

$$\gamma_f = \gamma^d{}_f + \gamma^p{}_f \quad (2)$$

where the $\gamma^d{}_l$ and $\gamma^p{}_l$ are the dispersive and polar components of surface energy of the liquid, respectively, and $\gamma^d{}_f$ and $\gamma^p{}_f$ are the dispersive and polar components of surface energy of the fiber, respectively. θ represents the contact angle at the fiber/liquid interface. Based on the above equations, the surface energy of three types of CFs was determined by averaging ten measurements.

Single fiber microbond test was performed to evaluate the interfacial shear strength (IFSS) between carbon fiber and epoxy matrix by pulling out a fiber from cured epoxy droplets (Fig. 2). The specimens were prepared by dripping epoxy resin droplets (the mixture of E51 and H256 in the weight ratio of 100:32) onto a carbon fiber monofilament with the embedded length of 60–80 μm using a fine-point applicator. The specimens were cured first at 80 °C for 1 h, second 120 °C for 2 h, and finally 150 °C for 3 h. Single fiber microbond test for the specimens was carried out on an interfacial microbond evaluation instrument (Tohei Sanyon

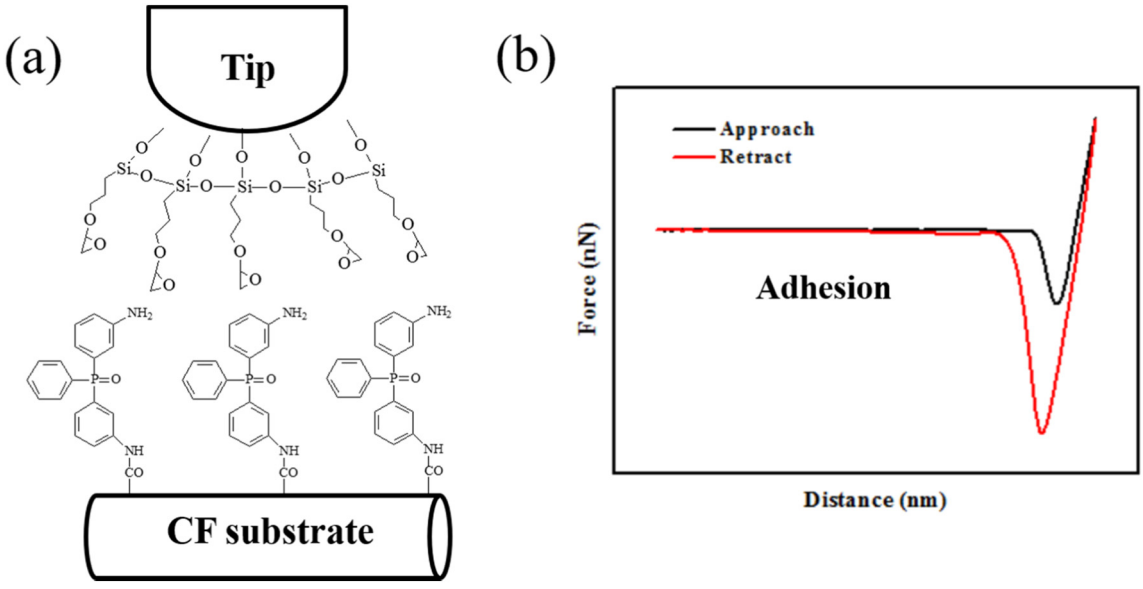

Fig. 1. Schematic diagram for the adhesion force measurement: (a) epoxy functionalized tip and BAPPO modified CF; (b) typical force-distance curves during the adhesion force measurement.

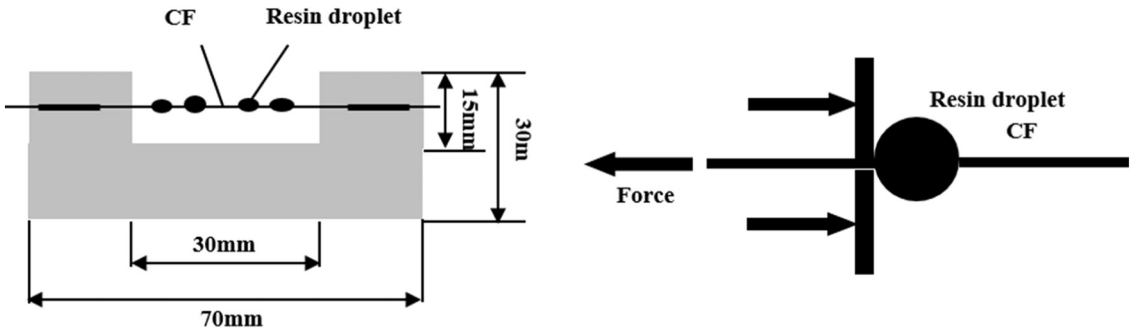

Fig. 2. Schematic illustration of single fiber microbond test.

Co., Ltd., Japan) at a crosshead displacement rate of 0.5 μm/s. The IFSS was calculated in accordance with Eq. (3):

$$\mathrm{IFSS} = F_{\max}/\pi dl \tag{3}$$

where F represents the maximum load; d represents the diameter of the carbon fiber; l represents the fiber length embedded in epoxy droplets. The recorded value of IFSS was obtained from the normal distribution of more than 100 measurements. Hereafter, the composite specimens with three types of CF are denoted as the as-received CF/EP, de-sized CF/EP and BAPPO-CF/EP, respectively.

3. Results and discussion

3.1. Characterization of three types of carbon fibers

As discussed in the experimental part, bis(3-aminophenyl) phenyl phosphine oxide (BAPPO) was synthesized via a two-step route. The dinitro compound, bis(3-nitrophenyl) phenyl phosphine oxide (BNPPO), was first synthesized via the nitration action of triphenylphosphine oxide (TPPO). Then, the obtained BNPPO was further hydrogenated to generate the diamine compound (BAPPO). Fig. 3(a) displays the FTIR spectra of TPPO, BNPPO and BAPPO. For TPPO, the characterization peaks of P—Ph and P═O appear at 1420 cm^{-1} and 1172 cm^{-1}, respectively. After the nitration action, two new absorption peaks located at 1513 cm^{-1} and 1332 cm^{-1} were observed, which are attributed to the Ph—NO_2 in BNPPO. After BNPPO was reduced to BAPPO, another two peaks at 3405 cm^{-1} and 3311 cm^{-1} were present assigned to the aromatic primary amine groups (—NH_2), while the characteristic absorption of nitro groups in BNPPO disappeared.

Fig. 3(b and c) presents ^{1}HNMR spectra of BNPPO and BAPPO, respectively. In Fig. 3(b), δ 2.5 ppm and δ 3.4 ppm represent the peaks of solvent dimethylsulfoxide and water; δ 8.5–8.4 ppm are the peaks of H proton at a, a′, b, b′ positions; δ 8.2–8.1 ppm refer to the peaks of H proton at d, d′ positions; δ 7.8–7.6 ppm are the peaks of H proton at c, c′, e, e′, f, f′, g positions. By comparison, a new peak located at δ 5.4 ppm was found in the spectra of BAPPO, which is attributed to the H proton at h, h′ position. Both the FTIR and ^{1}HNMR analysis confirmed

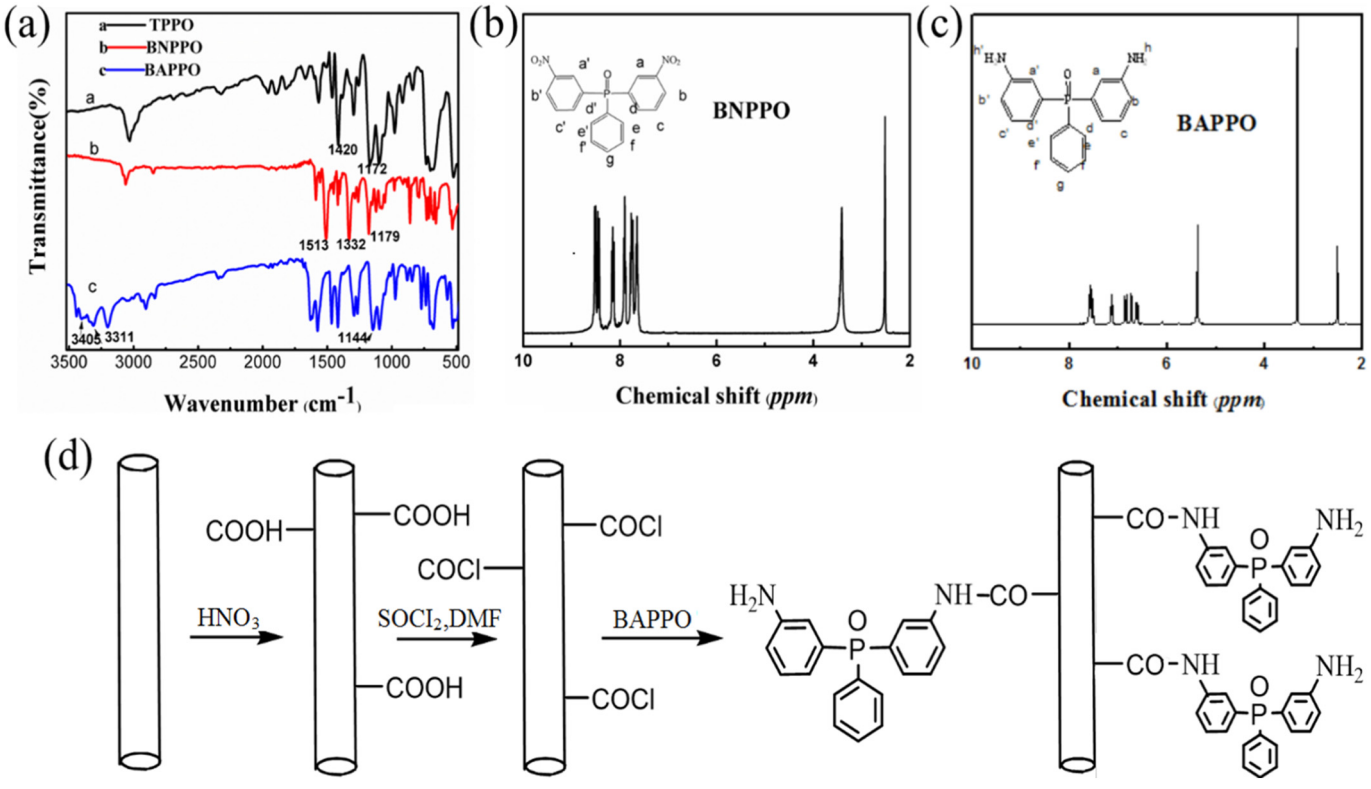

Fig. 3. (a) FT-IR spectra of TPPO, BNPPO, BAPPO; (b) ^{1}HNMR spectra of BNPPO and BAPPO; (c) schematic illustration of BAPPO chemically grafted on CF surfaces.

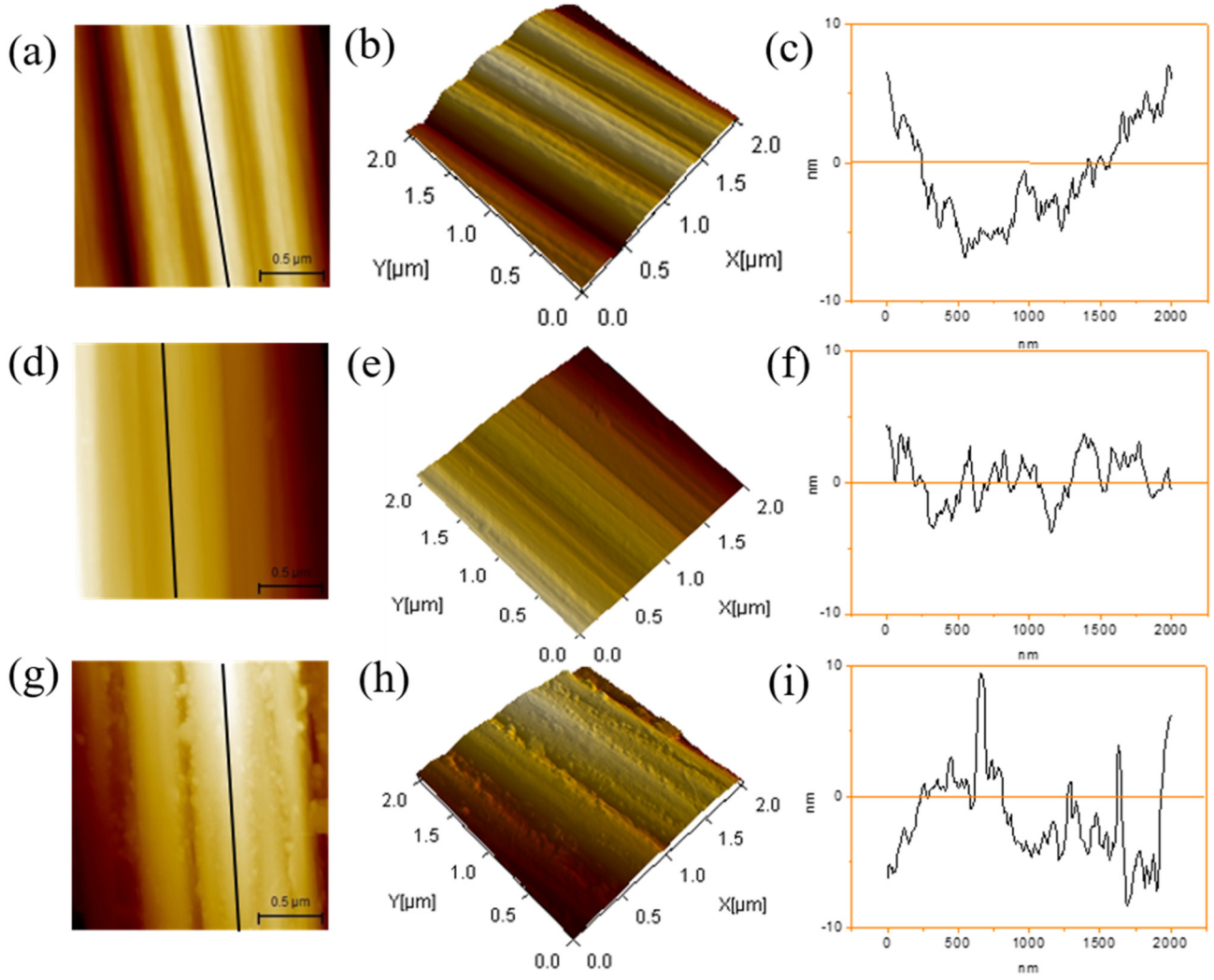

Fig. 4. AFM images of carbon fiber: (a–c) as-received CF; (d–f) de-sized CF and (g–i) BAPPO-CF. Left, 2D-topography; middle, 3D-topography; right, surface profile.

the successful synthesis of BAPPO, which was then used for modifying the CF through the amidation reaction (see Fig. 3(d)).

Fig. 4 shows the surface morphologies of as-received CF, de-sized CF and BAPPO modified CF. It was found that there are many intrinsic grooves on all the three kinds of CF surface resulting from the spinning process of the polyacrylonitrile precursor. Besides, some wrinkles are observed on the as-received CF surface along the fiber axis due to the existence of commercial sizing agent (see Fig. 4(b)). By contrast, the de-sized CF shown in Fig. 4(e) possesses a highly smooth surface since most of the commercial sizing agent was removed during the de-sized process, and the BAPPO modified CF possesses a much rougher surface than the as-received and de-sized CF, and some BAPPO particles were found to be evenly distributed on fiber surface (Fig. 4(h)), verified by the following XPS analysis.

The profiles of the three types of CF surfaces along the fiber axis (according to the black line in the left morphology) can also be found in Fig. 4. Compared to the as-received CF with an amplitude of around 12 nm, the de-sized CF has a relatively small amplitude of below 8 nm (see Fig. 4(f)). After the BAPPO modification, the amplitude of fiber surface increased to around 18 nm caused by the generation of BAPPO particles on the CF surface (see Fig. 4(i)).

Fig. 5 shows the XPS spectra of the as-received, de-sized and BAPPO modified CFs and Table 2 summarizes the relative concentration of compositional element of three types of CF samples. As shown in Table 2, the as-received CF has a great oxygen content of 24.8% resulting from commercial epoxy sizing agent. A significant decrease of the oxygen content is observed for the de-sized CF. At the same time, the O/C ratio drops from 0.3 to 0.2. These results demonstrate that most of the commercial sizing on the CF surface was removed during the de-sized process. As mentioned in the experimental section, before the introduction of BAPPO onto CF surface, the pretreatment of CF surface including oxidation and acyl chloride process was performed, and their XPS data are shown in Figs. S1, S2 and Table S1. It shows that the oxygen content in COOH-CF is much larger than that in the de-sized CF. On the other hand, the chlorine was detected in COCl-CF. When the CFs were modified with BAPPO, the oxygen concentration decreased sharply while the contents of C and N significantly increased. Meanwhile, the phosphorus appeared with a concentration of 4.0% in the BAPPO modified CF. XPS analysis confirmed that the three types of CFs have different surface chemistry, which would exist significant influence on the interfacial adhesion in the fiber-reinforced composites.

As known, the surface energy of the CF, especially its polar component, can significantly influence its wettability with the epoxy resin [27]. Generally, the CF with a large surface energy can be wetted easily by the epoxy. Table 3 displays the surface energy of as-received CF, de-sized CF and BAPPO-CF. Obviously, the de-sized CF has a lower surface energy (38.4 mN/m) in comparison with the as-received CF (45.0 mN/m). This is consistent with XPS analysis, in which the O

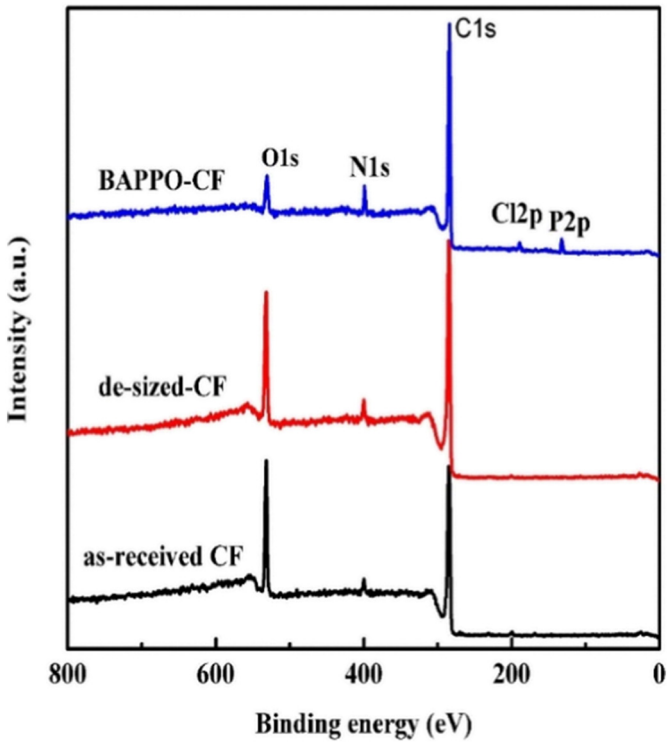

Fig. 5. XPS spectra of as-received CF, de-sized CF and BAPPO-CF.

content was reduced after the desized process. As a result, the polar component of surface energy decreased. However, a distinct increase to 55.0 mN/m is found for the surface energy of BAPPO modified CF due to the introduction of —NH_2 and other oxygen-containing functional groups during the pretreatment and subsequent BAPPO modification. BAPPO modified CF with a high surface energy could be wetted by epoxy resin more easily, compared to the as-received and de-sized CF.

3.2. Adhesion force measurement between CF and epoxy functionalized AFM tip

The adhesion forces between three types of CFs and the epoxy functionalized tip were measured by the PeakForce QNM AFM technique and they were expected to represent the interfacial interaction in CF/epoxy composites. The AFM images of the three types of CFs used in the adhesion force measurement are presented in Fig. 6(a–f), which are similar with the those presented in Fig. 4. The specific adhesion maps are also displayed in Fig. 6. Additionally, the representative force-replacement curves and the distribution of the adhesion force are given in Fig. 6(g–i) and (j–l).

As shown in Fig. 6(j–l), the adhesion forces between the as-received and de-sized CFs and the epoxy functionalized tip are around 22.5 nN and 17.9 nN, respectively, while the BAPPO-CF possesses a much larger adhesion force of 72.7 nN. Generally, there are two factors affecting the adhesion force between the sample surface and the tip. The first one is the surface properties of materials in contact with the tip, such as roughness, chemical heterogeneity and adsorption layer [28]. The second one is the interaction forces between the sample surface and the tip, such as van der Waals, electrostatics, capillary force, steric forces and forces due to chemical bonds or acid–base interactions, etc. [28,29]. For example, electrostatic forces exist on electrically charged surfaces and steric forces usually occur on polymers surfaces or some surfaces with properties similar to polymers [28,30]. The humidity dependent capillary force arises under ambient condition owing to the presence of a condensed meniscus of water between the tip and sample surface [31,32].

As mentioned in the experimental section, the adhesion force measurement experiments were conducted at a constant humidity. Therefore, the capillary forces are present between all the three CFs and the AFM tip. van der Waals forces widely exist and should be given by the Hamaker constants of AFM tip and CF samples and by the contact geometry. In these three cases, the difference of vdW attraction between the three types of CFs and tip could be neglected because the functionalized organic small molecules make little contribute on the van der Waals forces between fiber and tip. First, the contact area is small based on the diameter of tip (15 nm). Second, the Hamaker's constant of organic small molecules on CF surface are typically around $4–5 \times 10^{-20}$ J [33,34], which is almost an order of magnitude lower than that of CFs ($\sim 2.8 \times 10^{-19}$ J). These deductions were confirmed by the measured similar adhesion forces in the as-received and de-sized CF cases. The slight difference on the adhesion force in these two cases may result from the different surface roughness due to the existence of wrinkles on the as-received surface, as shown in Fig. 4.

By comparison, a much larger adhesion force of 72.7 nN is obtained between BAPPO-CF and the epoxy functionalized tip. This is due to the introduction of —NH_2 groups, which could react with epoxy groups on the functionalized tip, leading to the formation of hydrogen bonding and chemical bonding between the epoxy-functionalized tip and the BAPPO-CF (see Fig. 1) [35]. As a result, apart from the van der Waals and capillary force which are the two main interaction forces in the as-received CF and de-sized CF, the hydrogen and chemical bonding based interaction contributes to enhancement of the adhesion force between the epoxy-functionalized tip and the BAPPO-CF. Besides, considering the surface geometry, BAPPO-CF possesses a rougher surface with BAPPO particles on its surface as shown in Fig. 4, which could also lead to a larger adhesion force compared to that of the as-received and de-sized CF with relatively smooth surface.

3.3. Interfacial shear strength analysis of CF/epoxy micro-composites

The adhesion force measurement reflected the interfacial interaction between CFs and the epoxy functionalized tip on the nanoscale and molecular level, which can also be measured from the macro-scale in the CF/epoxy composites. To confirm this deduction, the single fiber microbond test based on the above three kinds of CFs and epoxy matrix was performed and the interfacial shear strength (IFSS) of three types of CF/EP micro-composites is shown in Fig. 7. It is found that the as-received CF/EP has a relatively high IFSS value of 79.6 MPa compared to the de-sized CF/EP with the IFSS of 74.1 MPa since the epoxy sizing on the as-received CF surface has a good compatibility with the epoxy resin due to their similar chemical structure. The de-sized CF surface consists of graphitic basal planes and edge sites, with a few small,

Table 2
Relative concentration of compositional element for CF samples.

Samples	Element composition (%)					O/C ratio
	C	O	N	P	Cl	
As-received CF	72.7	24.8	2.6	–	–	0.3
De-sized CF	78.1	18.3	3.6	–	–	0.2
BAPPO-CF	80.1	8.2	7.6	4.0	0.2	0.1

Table 3
Contact angle and surface energy of three types of CFs.

Samples	Contact angle (°)		Surface energy (mN/m)		
	Distilled water	Ethylene glycol	γ^d	γ^p	γ
As-received CF	57.5	47.8	5.9	39.1	45.0
De-sized CF	66.7	61.4	3.3	35.0	38.4
BAPPO-CF	48.2	40.8	4.5	50.6	55.0

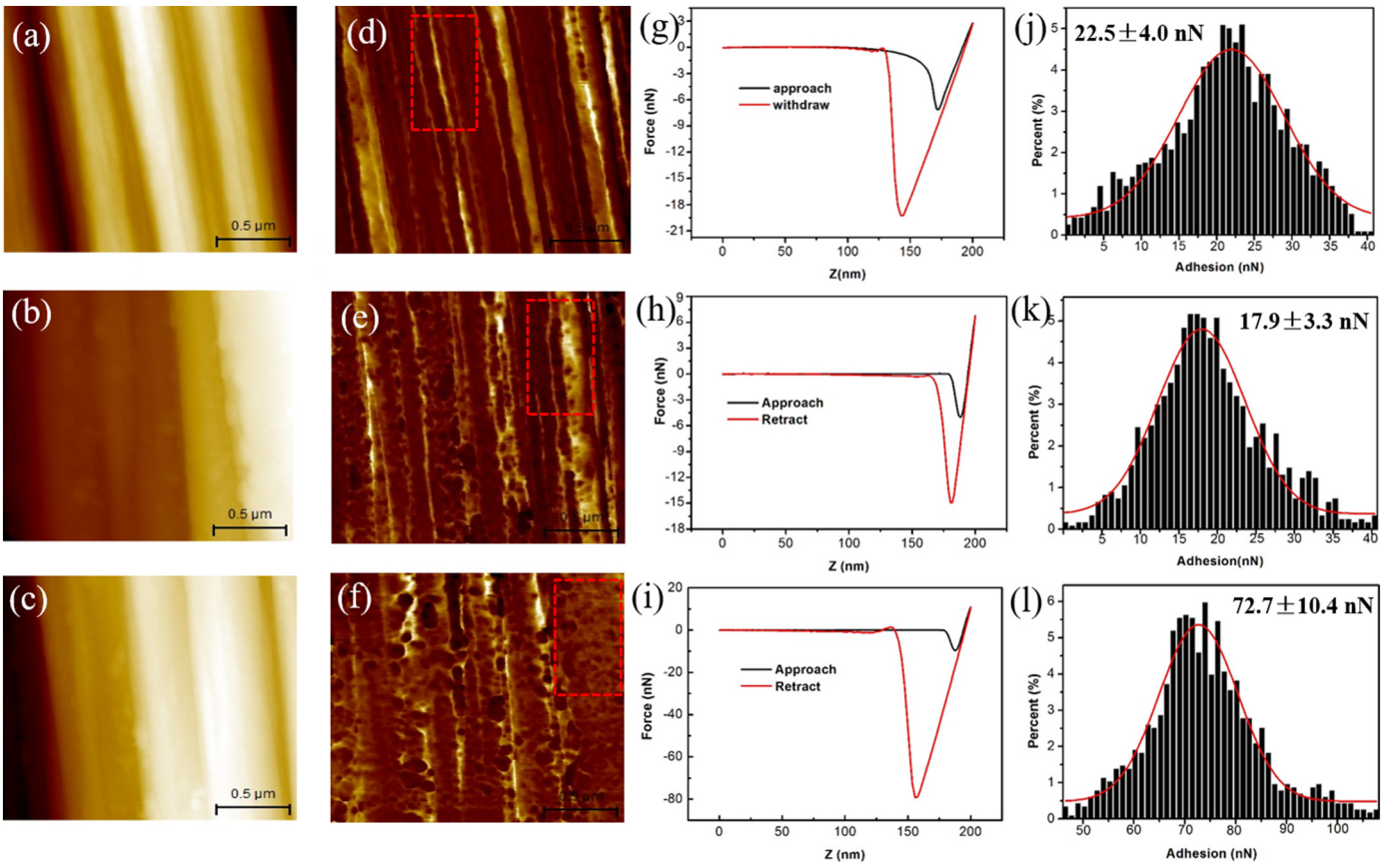

Fig. 6. Adhesion force measurement between the epoxy functionalized tip and CF samples. (a–c) AFM images of the as-received CF, de-sized CF and BAPPO-CF used in adhesion force measurement, respectively. (d–f) The corresponding adhesion maps of a–c. (g–i) The representative force-displacement curves during the adhesion force measurement process. (j–l) Histograms of the measured adhesion forces between the epoxy functionalized tip and CFs.

weakly bound crystallites left over from the graphitization process, making it suffer from low surface energy that can be found in Table 3. As a result, the de-sized CF is difficult to be wetted and chemically bonded with the epoxy matrix.

However, BAPPO-CF/EP has an IFSS value of 90.0 MPa, which is ~15% and ~22% larger than the as-received and de-sized CF/EP, respectively. This improvement could be attributed to: a) the increase of the wettability between the epoxy matrix and BAPPO-CF with a lot of oxygen-containing groups; b) the chemical bonding between the $-NH_2$ in BAPPO and epoxy groups during the curing of epoxy; c) the extra mechanical interlocking with the epoxy matrix resulting from the large surface roughness of the BAPPO-CF. As expected, these results are well consistent with the adhesion force obtained from the AFM measurement.

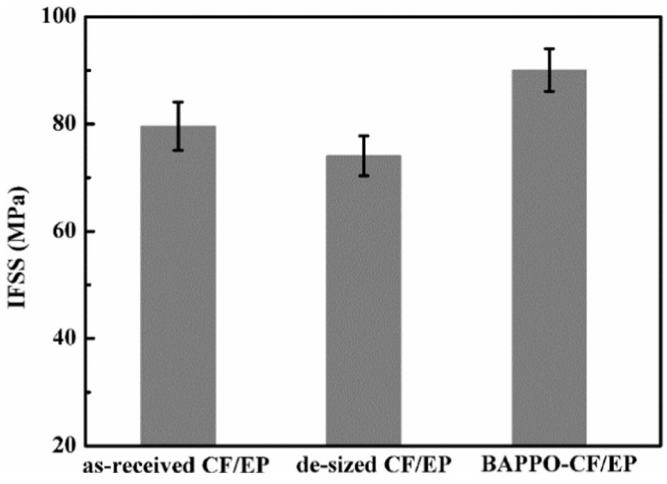

Fig. 7. Interfacial shear strength (IFSS) of the three types of CF/EP composites.

4. Conclusion

The present study contributes a new approach to investigate the interfacial adhesion in carbon fiber/epoxy composite by adhesion force measurement with the AFM. The results show that the BAPPO-CF possesses an adhesion force of 72.7 nN with the epoxy functionalized tip, which is 3 times larger than those of the as-received and de-sized CF. It can be explained by the formation of chemical bonding between the —NH_2 group in BAPPO and epoxy group on the functionalized tip. IFSS results from the traditional single fiber microbond test also show that the BAPPO-CF/EP has the highest IFSS of 90.0 MPa among the studied CF/EP composites. Both these two testing results demonstrate the direct influence of surface chemistry and morphologies of CFs on the interfacial adhesion. This study provides a new route to evaluate the interfacial interaction between CFs with different surface functional groups and the matrix, which can help optimize the performance of the carbon fiber reinforced composite from the aspect of molecular design.

Acknowledgements

This work was financially supported by Grant No. 51003019 from the National Natural Science Foundation of China.

Appendix A. Supplementary data

The Supporting information contains XPS spectra of COOH-CF and COCl-CF samples (Fig. S1); C1s curve fit spectra of carbon fibers (Fig. S2); Relative concentration of compositional atoms for CF samples (Table S1). Supplementary data to this article can be found online at https://doi.org/10.1016/j.matdes.2018.02.060.

References

[1] L. Liu, C. Jia, J. He, et al., Interfacial characterization, control and modification of carbon fiber reinforced polymer composites, Compos. Sci. Technol. 121 (2015) 56–72.
[2] M. Sharma, S. Gao, E. Mäder, et al., Carbon fiber surfaces and composite interphases, Compos. Sci. Technol. 102 (2014) 35–50.
[3] R.A. Jones, A. Cintora, R. White Scott, N.R. Sottos, Autonomic healing of carbon fiber/epoxy interfaces, ACS Appl. Mater. Interfaces 6 (2014) 6033–6039.
[4] S. Zhandarov, E. Mader, Peak force as function of the embedded length in pull-out and microbond tests: effect of specimen geometry, J. Adhes. Sci. Technol. 19 (2005) 817–855.
[5] N. Zheng, J. He, D. Zhao, et al., Improvement of atomic oxygen erosion resistance of carbon fiber and carbon fiber/epoxy composite interface with a silane coupling agent, Mater. Des. 109 (2016) 171–178.
[6] G. Lin, P. Geubelle, N. Sottos, Simulation of fiber debonding with friction in a model composite pushout test, Int. J. Solids Struct. 38 (2001) 8547–8562.
[7] C. Liang, J. Hutchinson, Mechanics of the fiber pushout test, Mech. Mater. 14 (1993) 207–221.
[8] Y.I. Yilmaz, Analyzing single fiber fragmentation test data by using stress transfer model, J. Compos. Mater. 36 (2002) 537–551.
[9] X.J. Gong, J.A. Arthur, L.S. Penn, Strain rate effect in the single-fiber-fragmentation test, Polym. Compos. 22 (2001) 349–360.
[10] B.W. Kim, J.A. Narin, Observations of fiber fracture and interfacial debonding phenomena using the fragmentation test in single fiber composites, J. Compos. Mater. 36 (2002) 1825–1858.
[11] Z. Zhao, K. Teng, N. Li, et al., Mechanical, thermal and interfacial performances of carbon fiber reinforced composites flavored by carbon nanotube in matrix/interface, Compos. Struct. 159 (2017) 761–772.
[12] D. Xia, S. Zhang, J.O. Hjortdal, et al., Hydrated human corneal stroma revealed by auantitative dynamic atomic force microscopy at nanoscale, ACS Nano 8 (2014) 6873–6882.
[13] F. Variola, Atomic force microscopy in biomaterials surface science, Phys. Chem. Chem. Phys. 17 (5) (2015) 2950–2959.
[14] M. Serri, M. Mannini, L. Poggini, et al., Low-temperature magnetic force microscopy on single molecule magnet-based microarrays, Nano Lett. 17 (3) (2017) 1899–1905.
[15] I. Sokolov, Q.K. Ong, H. Shodiev, et al., AFM study of forces between silica, silicon nitride and polyurethane pads, J. Colloid Interface Sci. 300 (2006) 475–481.
[16] M.E. Dokukin, I. Sokolov, Quantitative mapping of the elastic modulus of soft materials with HarmoniX and PeakForce QNM AFM modes, Langmuir 28 (46) (2012) 16060–16071.
[17] J. Colson, L. Andorfer, T.E. Nypelö, et al., Comparison of silicon and OH-modified AFM tips for adhesion force analysis on functionalised surfaces and natural polymers, Colloids Surf. A Physicochem. Eng. Asp. 529 (2017) 363–372.
[18] D. Alsteens, E. Dague, P.G. Rouxhet, A.R. Baulard, Y.F. Dufrene, Direct measurement of hydrophobic forces on cell surfaces using AFM, Langmuir 23 (2007) 11977–11979.
[19] B.D. Sattin, A.E. Pelling, M.C. Goh, DNA base pair resolution by single molecule force spectroscopy, Nucleic Acids Res. 32 (16) (2004) 4876–4883.
[20] M.A. Poggi, L.A. Bottomley, P.T. Lillehei, Measuring the adhesion forces between alkanethiol-modified AFM cantilevers and single walled carbon nanotubes, Nano Lett. 4 (1) (2004) 61–64.
[21] M. Seitz, C. Friedsam, W. Jöstl, et al., Probing solid surfaces with single polymers, Chem. Phys. Chem. 4 (9) (2003) 986–990.
[22] T. Hugel, M. Seitz, The study of molecular interactions by AFM force spectroscopy, Macromol. Rapid Commun. 22 (13) (2001) 989–1016.
[23] T. Jiang, Y. Zhu, Measuring graphene adhesion using atomic force microscopy with a microsphere tip, Nano 7 (24) (2015) 10760–10766.
[24] A. Noy, D.V. Vezenov, C.M. Lieber, Chemical force microscopy, Annu. Rev. Mater. Sci. 27 (1997) 381–421.
[25] F.L. Leite, P.S.P. Herrmann, Application of atomic force spectroscopy (AFS) to studies of adhesion phenomena: a review, J. Adhes. Sci. Technol. 19 (2005) 365–405.
[26] A. Kozbial, Z. Li, C. Conaway, et al., Study on the surface energy of graphene by contact angle measurements, Langmuir 30 (28) (2014) 8598–8606.
[27] J. Dong, C. Jia, M. Wang, et al., Improved mechanical properties of carbon fiber-reinforced epoxy composites by growing carbon black on carbon fiber surface, Compos. Sci. Technol. 149 (2017) 75–80.
[28] I.M. Pelin, A. Piednoir, D. Machon, et al., Adhesion forces between AFM tips and superficial dentin surfaces, J. Colloid Interface Sci. 376 (1) (2012) 262–268.
[29] H.J. Butt, B. Cappella, M. Kappl, Force measurements with the atomic force microscope: technique, interpretation and applications, Surf. Sci. Rep. 59 (1) (2005) 1–152.
[30] B.A. Patterson, U. Galan, H.A. Sodano, Adhesive force measurement between HOPG and zinc oxide as an indicator for interfacial bonding of carbon fiber composites, ACS Appl. Mater. Interfaces 7 (28) (2015) 15380–15387.
[31] T. Lai, P. Huang, Y. Cai, Adhesion reduction of diamond-like carbon films based on different contact geometries by using an AFM, J. Adhes. 92 (1) (2016) 18–38.
[32] Y. Sun, Y. Jiang, C.H. Choi, et al., Direct measurements of adhesion forces of water droplets on smooth and patterned polymers, Surf. Innov. (2017) 1–13.
[33] J.N. Israelachvili, Intermolecular and Surface Forces, 3rd ed. Academic Press Inc., San Diego, 2011.
[34] N. Zheng, Y. Huang, W. Sun, X. Du, et al., In-situ pull-off of ZnO nanowire from carbon fiber and improvement of interlaminar toughness of hierarchical ZnO nanowire/carbon fiber hydrid composite laminates, Carbon 110 (2016) 69–78.
[35] L. Ma, L. Meng, G. Wu, et al., Improving the interfacial properties of carbon fiber-reinforced epoxy composites by grafting of branched polyethyleneimine on carbon fiber surface in supercritical methanol, Compos. Sci. Technol. 114 (2015) 64–71.